J Solid State Electrochem (2002) 6: 367–373
DOI 10.1007/s10008-001-0260-5

ORIGINAL PAPER

Petr Krtil · Dina Fattakhova · Masahiro Yoshimura

Mechanism of soft solution processing formation of alkaline earth metal tungstates: an electrochemical and in situ AFM study

Received: 20 August 2001 / Accepted: 29 October 2001 / Published online: 8 December 2001

Abstract The mechanism of alkaline earth metal tungstate formation during soft solution processing was studied by cyclic voltammetry, electrochemical impedance spectroscopy and by direct in situ observation of the surface changes using atomic force microscopy. The electrochemical oxidation of W to WO_3 was followed by dissolution of WO_3 and, with some delay, by precipitation of tungstates at the metal surface. The same Tafel slopes observed in Li^+, Ba^{2+}, Sr^{2+} and Ca^{2+} containing solutions indicate that the course of the oxidation process is independent of the cation present in solution. The observed differences in the current-voltage curves outside the Tafel region are accounted for by the different film-forming tendencies of the various alkaline earth metal cations. The growth of tungstate layers at the W substrate decreases the electrochemically active area and limits the production of WO_4^{2-} at later stages of deposition. At low potentials ($E < 0.2$ V) the oxidation of W is the rate-controlling step. At higher potentials, however, the dissolution process slows down due to a relative decrease of the pH in the electrode vicinity and dissolution becomes the rate-limiting step.

Keywords Atomic force microscopy · Tungstates · Thin film deposition

Introduction

Soft solution processing (SSP) is one of the recent trends in the synthesis of advanced inorganic materials with controlled properties [1, 2]. By the term SSP we understand in this case the hydrothermal or electrochemical-hydrothermal treatment of starting materials to obtain the final product in a desirable shape. The preparation of double oxide thin films at a metal substrate is an example of the convenience of this processing. This method was successfully used to prepare materials like, for example, $SrTiO_3$ [3, 4], $BaTiO_3$ [5], $LiNiO_2$ [6, 7] and other materials, at temperatures below 200 °C. From the mechanistic point of view these processes can be described as oxidation of a transition metal followed by dissolution of the transition metal oxide and finally by crystallization (precipitation) of the double oxide from solution. The latter two steps may be considered as chemical ones. Anodic oxidation of a transition metal is, however, a complex process, the description of which is difficult, particularly at elevated temperatures (i.e. under hydrothermal conditions). This is also the reason why direct experimental confirmation of the proposed mechanism for film formation is lacking for most of the systems so far and no attempts to quantify the film formation process have been made.

The immediate goal of this study was to use an appropriate model system which would allow us to verify the proposed mechanism and to characterize the electrochemical and chemical parts of the process in terms of rate-controlling steps.

To avoid problems with instrumentation, we sought a metal/double oxide system proceeding at low temperature. Also the kinetics of film formation in the model system should be sufficiently fast to obtain compatible experimental timescales for both the method and the deposition process. Among several systems meeting the above-mentioned criteria, we selected the alkaline earth metal tungstates for this study. These materials can be prepared at room temperature on the timescale of 10^2–10^3 s [8, 9, 10], which allows us to employ various electrochemical as well as in situ non-electrochemical approaches to describe the film formation. In this paper we present the results of cyclic voltammetry and electrochemical impedance spectroscopy

P. Krtil (✉) · D. Fattakhova
J. Heyrovský Institute of Physical Chemistry,
Dolejškova 3, Prague 8, Czech Republic
E-mail: Petr.Krtil@jh-inst.cas.cz

P. Krtil · M. Yoshimura
Materials and Structures Laboratory,
Tokyo Institute of Technology,
4259 Nagatsuta, Midori, Yokohama 226, Japan

(EIS), together with in situ atomic force microscopy (AFM) at constant potential to characterize the tungstate formation.

Experimental

Electrochemical experiments were carried out in a one-compartment glass cell, using a PAR 273 potentiostat complemented in impedance measurements by an EGG 5210 lock-in amplifier. Tungsten foil (0.2 mm thick, Nilaco, 99%) was used as a working electrode. All potentials were measured and are quoted with respect to an Ag/AgCl reference electrode; the three-electrode arrangement was complemented by a platinum auxiliary electrode. EIS was measured in the frequency range 100 kHz to 5 mHz with an a.c. amplitude of 10 mV (peak to peak). The electrode was subjected to a potentiostatic oxidation at 0.0 V for 5–40 min followed by an open circuit equilibration for 20 min prior to impedance measurement. Measured impedance data were analyzed by non-linear least-square (NLLS) fitting using Z-Plot/Z-View software (Scribner Associates).

The in situ AFM observations of the working electrode surface changes were carried out using a Pico scanning probe microscope (Molecular Imaging) working in contact AFM mode (Si_3N_4 cantilever; force constant 0.12 N/m). A Pico potentiostat (Molecular Imaging) was used for polarization of the working electrode during the AFM scanning. Owing to the geometric restrictions, the Ag/AgCl reference electrode was substituted with a silver wire pseudo-reference electrode (PRE) in electrochemical AFM experiments. The potential of the Ag PRE was then quoted with respect to Ag/AgCl and the potentials were recalculated to the Ag/AgCl scale. Measurements were carried out in a solution containing 10^{-2} mol/L $M(OH)_2$ (M = Ba, Sr or Ca) (all p.a. grade Kanto Chemicals) and 10^{-1} mol/L $NaClO_4$ (p.a. grade Wako Chemicals) as a supporting electrolyte. For experiments in a Li-containing solution, LiOH (p.a. grade Wako Chemicals) in the same concentration was used instead of the alkaline earth metal hydroxides. All solutions were prepared using double distilled water, which was purged with Ar for 1 h to remove dissolved CO_2 and oxygen. The electrolyte solutions were kept under Ar prior to use.

Results and discussion

The anodic behavior of tungsten electrodes in alkaline media has been covered in several papers [11, 12, 13, 14]. The overall process is described by the following equation:

$$W(s) + 8OH^-(aq) \rightarrow WO_4^{2-}(aq) + 4H_2O + 6e^- \qquad (1)$$

Detailed analysis expects the whole process to be composed of four electrochemical and one chemical steps [14]. The dissolution rate of tungsten is proportional to the pH [11, 12] and is independent of the concentration of WO_4^{2-} in solution [14]. Cyclic voltammograms taken on a W electrode in the presence of some alkaline and alkaline earth metal cations are shown in Fig. 1. The voltammetric curve measured in Li^+ containing solution (where no double oxide film is formed) exhibits three pronounced current maxima at –206, 120 and 520 mV. The presence of several current peaks shows the complexity of the whole anodic process. According to quartz crystal microbalance (QCM) data [16], the peaks do not represent definite steps of the whole six-electron transfer, but appear rather due to an oxide accumulation at the electrode surface which proceeds at positive potentials [11, 12, 13]. This is caused by slowing of the WO_3 dissolution owing to the relative lack of OH^- in the electrode vicinity. Since the oxidation state of tungsten in this surface layer can be lower than VI, one can assign the positive current maxima to the oxidation of the previously accumulated oxide to oxidation state VI.

Cyclic voltammograms taken in the presence of alkaline earth metal cations differ for Ca^{2+}, Ba^{2+} or Sr^{2+} containing solutions. While in the case of Ca^{2+} the measured voltammogram shape shows a good agree-

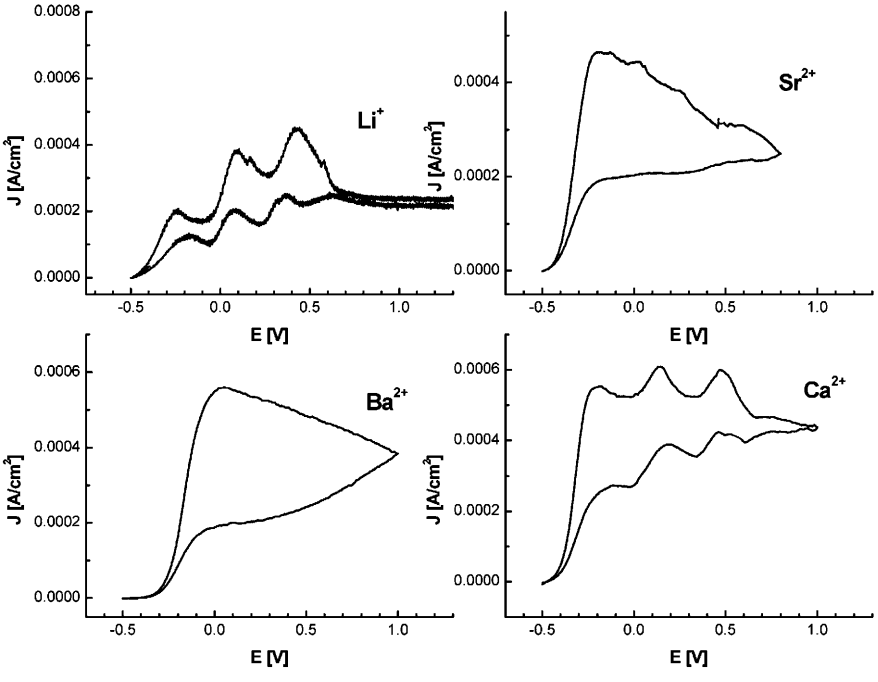

Fig. 1 Cyclic voltammograms of the tungsten electrode in solutions containing 0.01 mol/L Li^+, Ba^{2+}, Sr^{2+} or Ca^{2+} in 0.1 mol/L $NaClO_4$; scan rate 3 mV/s

ment with that observed in the Li^+ containing solution, the voltammogram shapes recorded in Ba^{2+} or Sr^{2+} containing solutions show significant differences. There is only one peak in the voltammogram, which in the case of Ba^{2+} containing solutions appears at ca. 200 mV more positive potential with respect to the most negative peak than in the case of Li^+ or Ca^{2+} containing solutions. The absence of the other peaks can be explained by formation of a tungstate at the electrode surface. This decreases the electrochemically active area of W metal so the WO_x accumulation is suppressed. In the presence of an alkaline earth metal cation, the formation of a tungstate proceeds according to Eq. 2:

$$WO_4^{2-}(aq) + M^{2+}(aq) \rightarrow MWO_4(s) \quad (2)$$

where M is Ba^{2+}, Sr^{2+} or Ca^{2+}. The difference in the cyclic voltammograms taken in Ba^{2+}, Sr^{2+} or Ca^{2+} containing solutions we attribute to the different kinetics of tungstate crystallization. This explanation seems to be supported also by Tafel plots (see Fig. 2) extracted from slow linear sweep voltammetry ($v \approx 0.2$ mV/s). The log(J) vs. E curves measured for different cations show similar patterns. They can be divided into two parts. The first part – at low potentials (i.e. potentials negative to ca. –75 mV) – is characterized by a linear dependence of log(J) on the potential, as predicted by the Tafel equation. This means that the charge transfer reaction is the rate-limiting step. The slope of this dependence was used to estimate the number of electrons involved in the rate-limiting electrode reaction, n_a. This value was for all cations close to 1, corresponding with literature data previously published on the system [14] (see Table 1). In the other part of the curve (i.e. at potentials positive to

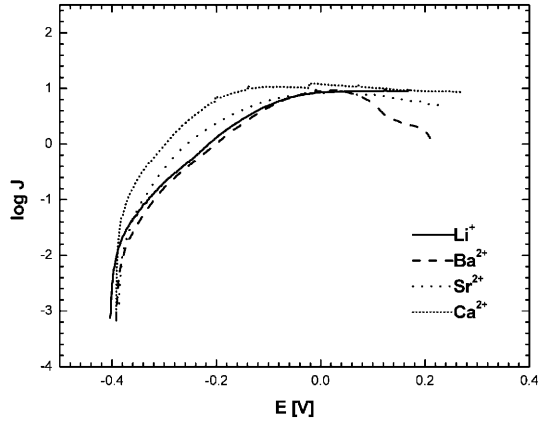

Fig. 2 Tafel plots of the tungsten electrode in solutions containing 0.01 mol/L Li^+, Ba^{2+}, Sr^{2+} or Ca^{2+} in 0.1 mol/L $NaClO_4$. Data were taken from slow scan polarization at a scan rate of ca. 0.2 mV/s

Table 1 The numbers of electrons exchanged in the rate-limiting electrochemical process for different cations

Cation	n_a
Li^+	1.02
Ba^{2+}	1.08
Ca^{2+}	1.09
Sr^{2+}	1.22

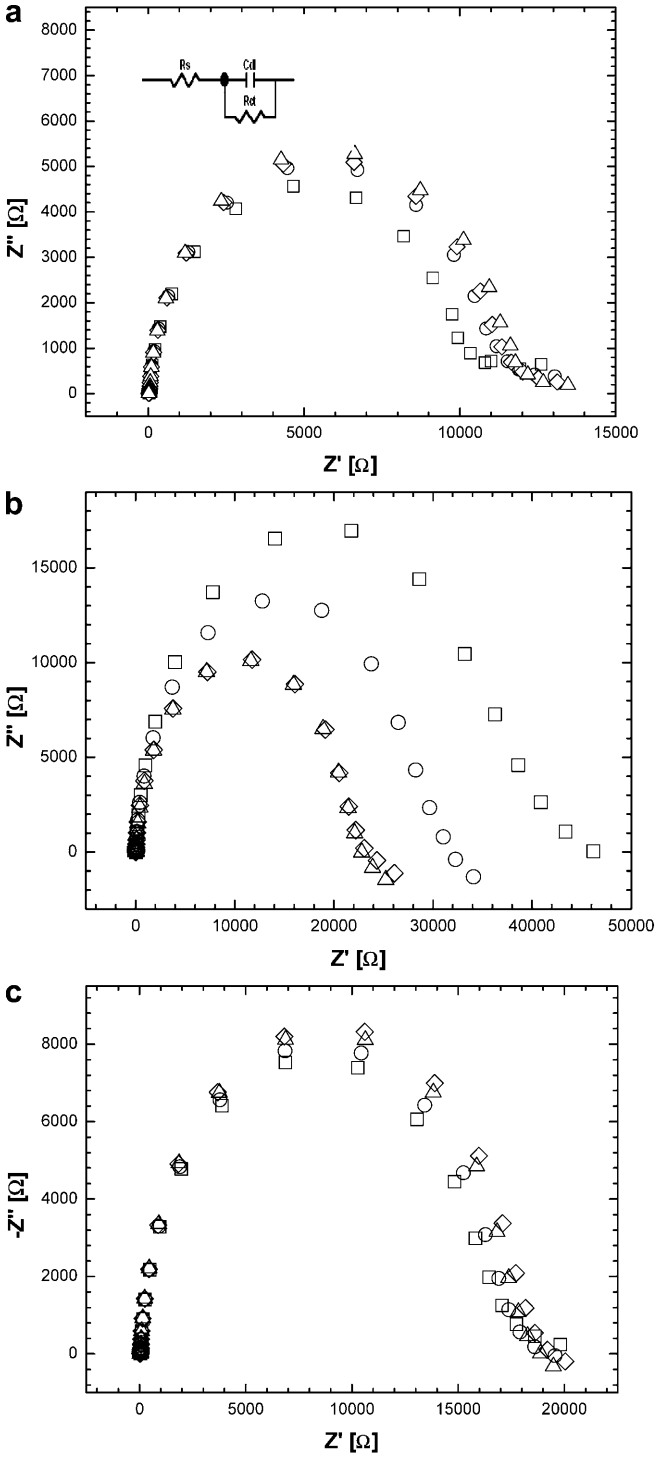

Fig. 3 Impedance spectra of a tungsten electrode polarized for different times at 0 V in Li^+ (**a**), Ba^{2+} (**b**) and Sr^{2+} (**c**) containing solutions. The duration of potentiostatic oxidation preceding the impedance measurements was 5 min (*open squares*), 10 min (*open circles*), 15 min (*open diamonds*) or 20 min (*open triangles*)

–75 mV) the logarithm of the current density is independent of the potential in Li^+ containing solutions. On the other hand, in the presence of any alkaline earth metal cation the log(J) signal decreases with increasing potential. The current density decrease can be assigned, for example, to a decrease of the active electrode area owing to the deposition of an insulating tungstate layer at the surface. Different rates of log(J) decay should then reflect different rates of tungstate formation for different alkaline earth metals.

Electrochemical impedance data measured at open circuit conditions complement the information extracted from voltammetry (see Fig. 3). The impedance form depressed semicircular spectra in a complex impedance plane and can be fitted with the equivalent circuit shown in the inset of Fig. 3a. Resistor R_s, which represents the high-frequency intercept of the semicircle with the real axis, represents the overall resistance of the electrolyte solution. The parallel combination of the resistor R_{ct} and capacitor C_{dl} represent the resistance connected with the charge transfer reaction and the electrode double layer capacitance, respectively.

Low values of R_s ranging between 4 and 8 Ω/cm^2 for all measured cations reflect good compensation of the solution resistance. The specific double layer capacitance calculated for the geometric area of the electrode, found using NLLS fitting, was between 50 and 70 $\mu F/cm^2$. The observed values agree well with values generally expected for solid electrodes. Such agreement points towards low roughness of the tungsten samples (see below).

While general impedance patterns of the W electrode in different solutions before anodization do not show significant differences, the electrode impedance after polarization at 0 V follows in fact two different tendencies. In the case of tungsten oxidation in Li^+ containing solutions, one may observe an increase of the depressed semicircle with increasing oxidation time (see Fig. 3a). Approximately 30 min potentiostatic oxidation leads to an increase of both R_{ct} and C_{dl} by ca. 13%. A comparable increase of the tungsten area was observed also in AFM measurements.

An opposite tendency was found in the behavior of a W electrode oxidized in Ba^{2+} containing solutions. In

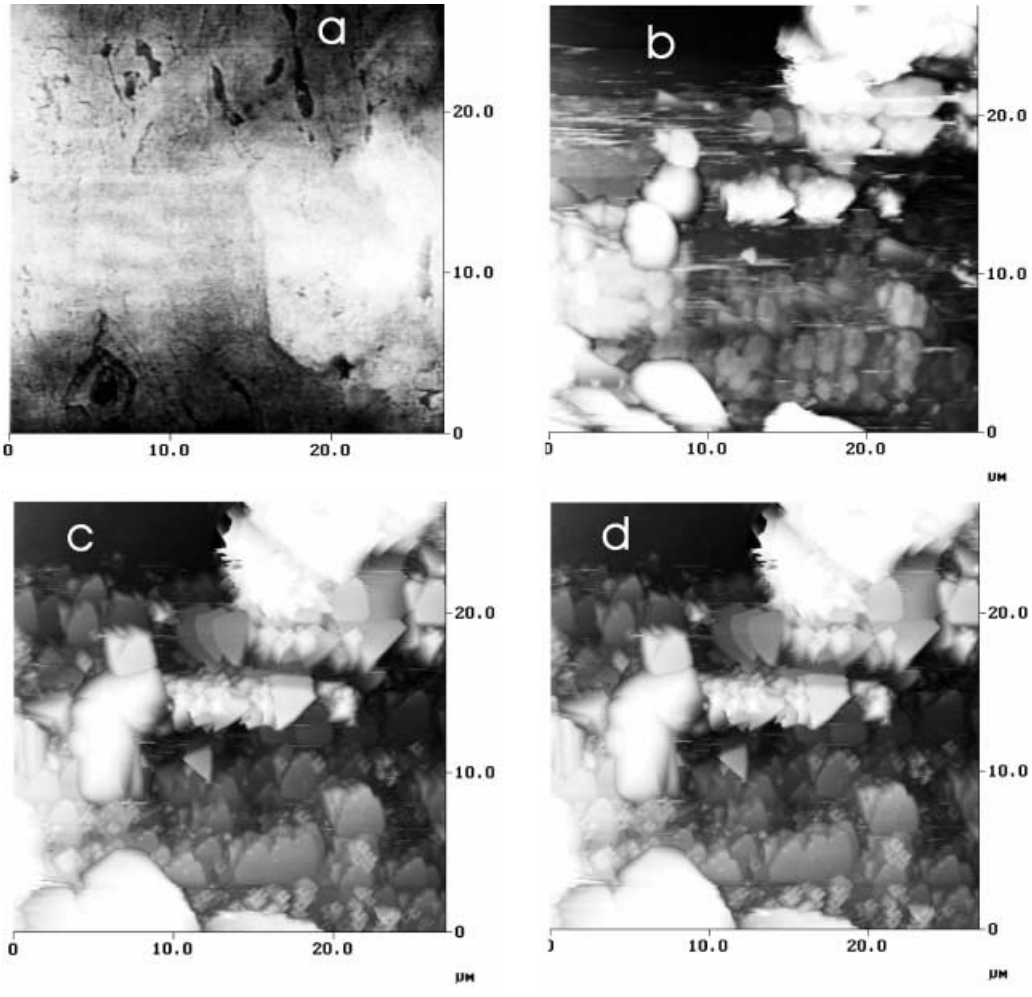

Fig. 4a–d AFM images of the tungsten electrode surface acquired in situ during deposition of a $BaWO_4$ film by potentiostatic oxidation of a tungsten electrode in Ba^{2+} containing solution at pH 12 and 0 V. Images were taken before (**a**) and 720 s (**b**), 3000 s (**c**) and 5400 s (**d**) after potential application

this case we experienced an increase of double layer capacitance C_{dl}, similar to that observed in Li^+ containing solutions. The capacitance increase of ca. 20% was accompanied by about a 40% decrease of R_{ct}. We believe that the decrease of the polarization resistance is connected with deposition of electrochemically inactive $BaWO_4$ at the electrode surface. This leads to a decrease of the electrochemically active area so if the exchange current density remains constant the observed R_{ct} ought to decrease. The formation of a new phase at the electrode surface increases the electrode total area, reflected in the increase of C_{dl}. It is necessary to note that all significant changes of impedance spectra were observed for variations of the deposition time between 0 and 25 min. Prolongation of oxidation time beyond 25 min does not cause any further change of the electrode impedance, so one can assume that the formation of the tungstate film is completed, or at least slowed down.

Impedance behavior of tungsten electrodes oxidized in Sr^{2+} containing solutions tracks that observed in Li^+ containing solutions for short polarization times ($t < 25$ min). At higher polarization times the mechanism observed in Ba^{2+} containing solutions prevails. Impedance characteristics of the electrodes polarized in Ca^{2+} containing solutions show qualitatively good agreement with the type of behavior observed in Li^+ containing solutions.

As has been demonstrated above, the electrochemical data show that the formation of tungstates is controlled by the chemical part of the process. A clearer visualization of the process, however, can be obtained using direct observation of the electrode surface during the deposition process by means of AFM.

Images of the tungsten electrode surface obtained in situ during potentiostatic preparation of $BaWO_4$ and $SrWO_4$ at 0 V are shown in Figs. 4 and 5, respectively. It is necessary to note that the roughness of the tungsten substrate surface is not negligible on the scale of the measurement (27×27 μm) (see Figs. 4a and 5a). The average roughness of the surface before oxidation was about 30 nm, which indicates surface inhomogeneity. The dissolution of the tungsten surface proceeds unevenly: a higher resulting solution concentration of WO_4^{2-} can be expected near the edges of surface scratches. These locations can be also considered as preferential sites where heterogeneous nucleation may occur. This tendency is well documented in Figs. 4b and 5b. The formation of crystals (surprisingly large in the case of $BaWO_4$) is evident at designated places within ca. 3 or 10 min for $BaWO_4$ and $SrWO_4$, respectively. These

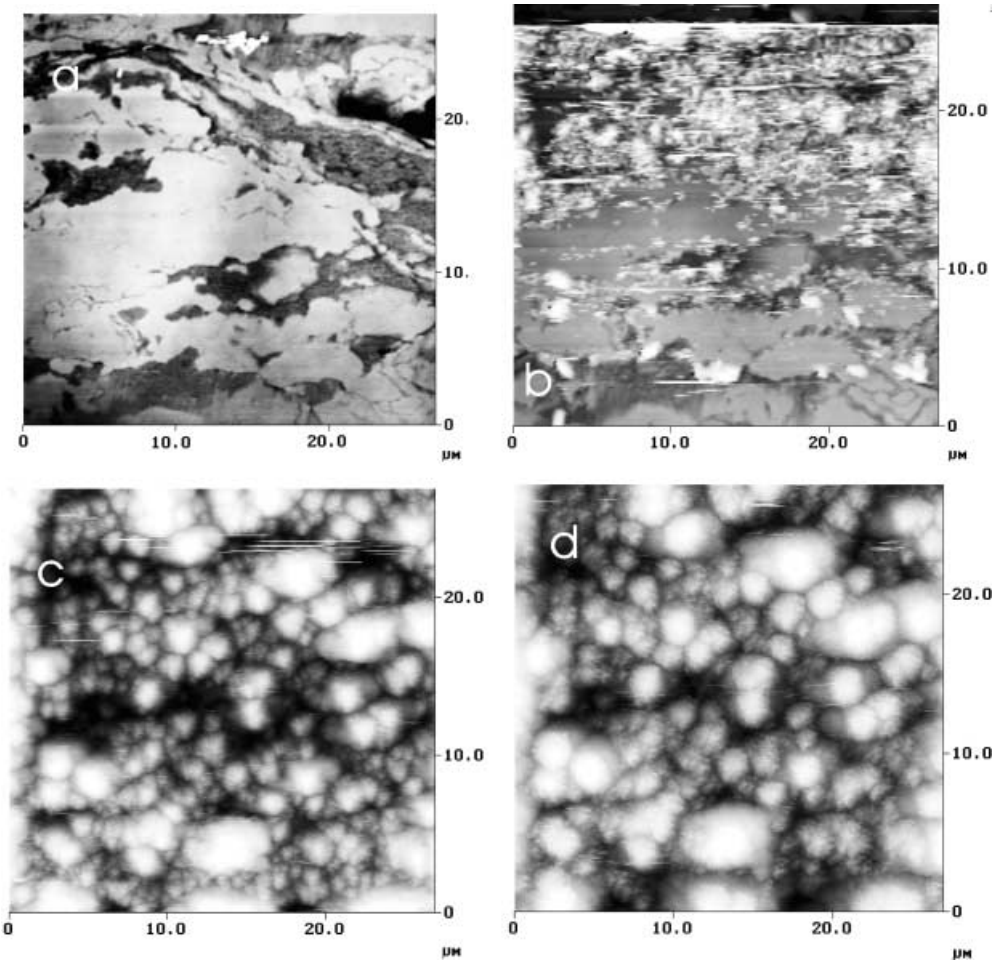

Fig. 5a–d AFM images of the tungsten electrode surface acquired in situ during deposition of a $SrWO_4$ film by potentiostatic oxidation of a tungsten electrode in Sr^{2+} containing solution at pH 12 and 0 V. Images were taken before (**a**) and 720 s (**b**), 1440 s (**c**) and 2700 s (**d**) after potential application

time responses are slightly lower than those one may extract from, for example, impedance or QCM measurements [15, 16]. Unfortunately, we cannot decide conclusively about the character of the nucleation process, since we cannot omit the effect of cantilever friction. Tungstate anions produced by further polarization are consumed either by growth of the primarily formed crystals or they cause formation of new crystals, which are smaller than those formed initially (see Figs. 4c, d and 5c, d). $BaWO_4$ formation can also be observed using in situ AFM at higher potentials (E up to 0.5 V); $SrWO_4$ formation, on the other hand, is suppressed in AFM observations at higher potentials.

Semi-quantitative analysis of the AFM images taken during formation of $BaWO_4$ and $SrWO_4$ shows the difference in kinetics as well in thermodynamics of both processes (see Fig. 6a and b). As shown by the average and maximum roughness signals, crystal formation of $SrWO_4$ is delayed with respect to $BaWO_4$. Since we know that the electrochemical part of the process is virtually the same for both systems, we can also easily anticipate similar populations of WO_4^{2-} in solution at the early stage of potentiostatic polarization. The initial delay before formation of the first crystals was observed corresponds to a period necessary to achieve a sufficient concentration of WO_4^{2-} for precipitation to proceed. The driving force for both phases of the crystallization process (nucleation and growth) is governed by the supersaturation ratio α, which can be (with certain simplification) defined as follows:

$$\alpha = \frac{c}{c*} \tag{3}$$

where c is actual solute concentration and c^* is the equilibrium solubility of the solute. In our case we can take advantage of the rather limited solubility of the tungstates and express the supersaturation using the solubility product:

$$\alpha = \frac{c_{WO_4^{2-}} c_{M^{2+}}}{c_s} \tag{4}$$

where M is alkaline earth metal and c_s is the corresponding solubility product. Though the solubility products for alkaline earth metals are not known (except for $CaWO_4$), a general tendency of decreasing solubility on going from Ca to Ba can be expected [16]. This is probably the reason for the different result for the behavior of the W electrode in Ba^{2+} and Sr^{2+} containing solutions at higher potentials (positive to 0.5 V) in the AFM arrangement. At high potentials the concentration of WO_4^{2-} in solution becomes controlled by WO_3 dissolution, i.e. it is not proportional to passed charge. Therefore the $BaWO_4$ solubility product is sufficiently small such that an α value higher than 1 can be obtained under these conditions. On the other hand, the crystallization of $SrWO_4$ is hindered since the WO_4^{2-} concentration needed to obtain $\alpha > 1$ is higher than the actual one controlled by WO_3 dissolution (note that the alkaline earth metal cation concentrations are the same for both Ba^{2+} and Sr^{2+} containing solutions).

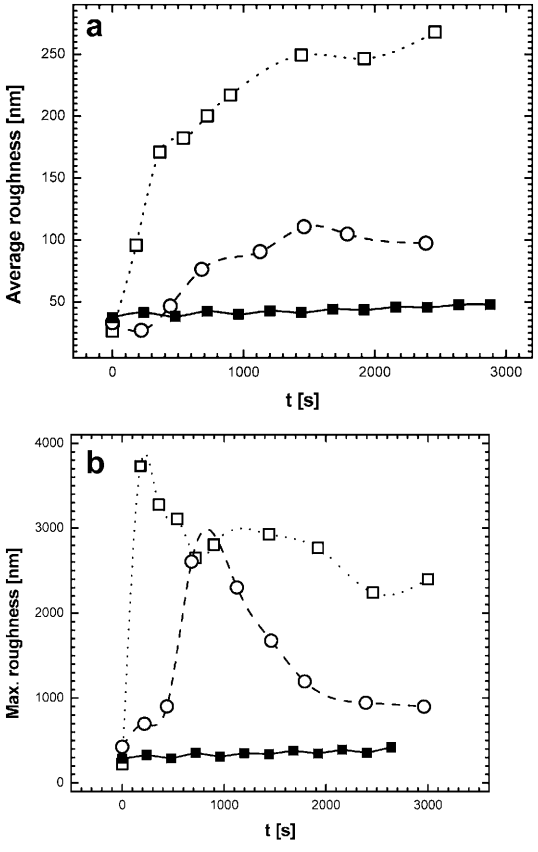

Fig. 6 Time dependence of the average roughness (**a**) and maximum roughness (**b**) of the tungsten electrode surface when oxidized in Ba^{2+} containing (*open squares*), Sr^{2+} containing (*open circles*) and in Li^+ containing (*filled squares*) alkaline media at pH 12 and 0 V. Values were extracted from in situ AFM experiments

Conclusions

A combination of electrochemical data with in situ AFM observations of the substrate surface are capable of providing direct evidence for the expected mechanism of alkaline earth metal tungstates formation. At low potential the crystallization is the rate-limiting step, so the film formation tendency may be expressed in terms of solubility products. However, at increased potentials the dissolution of WO_3 becomes the rate-controlling step. Unfortunately, the experimental approach adopted in this study provides rather semi-quantitative information, and cannot be used to determine, for example, solubility products or to calculate the growth rates of the tungstate films at different deposition conditions.

Acknowledgements This work was supported by the Japan Society for Promotion of Science under the contract "Research for the Future" no. 96R06901. D.F. appreciates financial support from the Grant Agency of the Czech Republic under contract 203/99/0879.

References

1. Yoshimura M (1998) J Mater Res 14:796
2. Yoshimura M, Suchanek W, Han KS (1999) J Mater Chem 9:77
3. Kajiyoshi K, Tomono K, Hamaji Y, Kasanami T, Yoshimura M (1996) J Am Ceram Soc 79:613
4. Kajiyoshi K, Yoshimura M, Hamaji Y, Tomono K, Kasanami T (1996) J Mater Res 11:169
5. Bacsa R, Ravidranathan P, Dougherty JP (1992) J Mater Res 7:423
6. Han KS, Tsurimoto S, Yoshimura M (1999) Solid State Ionics 121:229
7. Han KS, Krtil P, Yoshimura M (1998) J Mater Chem 8:2043
8. Cho WS, Yashima M, Kakihana M, Kudo A, Sakata T, Yoshimura M (1995) Appl Phys Lett 66:1025
9. Cho WS, Yashima M, Kakihana M, Kudo A, Sakata T, Yoshimura M (1996) Appl Phys Lett 68:137
10. Cho WS, Yoshimura M (1996) Jpn J Appl Phys 35:L1449
11. Heumann Th, Stolica N (1971) Electrochim Acta 16:643
12. Heumann Th, Stolica N (1971) Electrochim Acta 16:1635
13. Armstrong RD, Edmundson K, Firman RE (1972) J Electroanal Chem 40:19
14. Kelsey GS (1977) J Electrochem Soc 124:814
15. Krtil P, Yoshimura M (1998) J Solid State Electrochem 2:321
16. Krtil P, Nishimura S, Yoshimura M (1999) Electrochim Acta 44:3911